Interaction Between the Fluorinated Amphiphilic Copolymer Poly(2,2,3,4,4,4-hexafluorobutyl methacrylate)-*graft*-Poly(SPEG) and DNA

Ling Li,[1] Shengdong Xiong,[1] Yingxi Wang,[1] Gongwu Song,[1] Shuilin Wu,[1,2] Paul K. Chu,[2] Zushun Xu[1,2]

[1]*Key Laboratory for the Synthesis and Application of Organic Function Molecules (Ministry of Education), Hubei University, Wuhan 430062, China*
[2]*Department of Physics and Materials Science, City University of Hong Kong, Tat Chee Avenue, Kowloon, Hong Kong, China*

Received 14 November 2009; accepted 19 February 2010
DOI 10.1002/app.32339
Published online 19 May 2010 in Wiley InterScience (www.interscience.wiley.com).

ABSTRACT: A synthesized copolymer, synthesized from HFMA (hexaflurobutyl methacrylate) and SPEG (PHFMA-*g*-PSPEG), was synthesized. PHFMA-*g*-PSPEG intercalated to the DNA base pair via a strong hydrophobic force, and this was conformed by ultraviolet spectroscopy, transmittance measurements, micropolarity measurements, resonance light scattering (RLS) spectroscopy, and particle size measurements. The copolymer was used as a new probe to detect DNA according to the RLS technique. The hydrophobic interaction between PHFMA-*g*-PSPEG and DNA significantly enhanced the RLS signal, and the enhanced RLS intensity at 422 nm was proportional to the nucleic acid concentration within the range of 0.09–0.90 mg/L with a detection limit (3σ) of 4.0 μg/L.
 J Appl Polym Sci 118: 291–298, 2010

Key words: biological applications of polymers; drug delivery systems; fluoropolymers

INTRODUCTION

Studies of gene delivery have attracted much attention because of its potential applications in the treatment of a variety of diseases.[1,2] A number of gene carriers, including viral and nonviral vectors, have been proposed to increase the efficiency of gene delivery. However, clinical applications of viral vectors are limited by their inherent disadvantages, such as immunogenicity, the contamination of the helper virus, the limited size of the inserted DNA, and the risk of integration into the host's genome.[3,4] Cationic polymers are believed to be effective nonviral vectors, and there has been a great deal of study on the interactions between synthetic cationic polymers and DNA.[5,6] Nonetheless, the efficiency of gene delivery using cationic polymers that are not biodegradable is limited. Recently, applications of biodegradable nonionic polymers to gene delivery have attracted significant attention because of their superior biocompatibility[7] and biodegradability, which contribute to lower toxicity in comparison with nondegradable polymers.[8–11] Nonionic polymers have a degradable ester backbone, and its degradability has been well demonstrated.[12,13] The use of nonionic polymers with a degradable ester backbone should provide a safer gene delivery approach for curing diseases.

At the same time, the interactions between DNA and surfactants, which have been studied extensively in recent years,[14–18] are very important in biotechnological and biomedical applications, particularly in *in vivo* gene delivery and gene transfer.[19,20] Amphiphilic copolymers consisting of long hydrophobic and hydrophilic chains with a high molecular weight greater than 1000 are considered to be macromolecular surfactants. Because of their viscosity and surface activity, amphiphilic copolymers are widely used in gel formers, surface modifiers, foam and colloid stabilizers, thickeners, wetting agents, compatibilizers, microreactors, and nanostructured materials.[21] Poly(ethylene glycol) (PEG) is widely used as the hydrophilic side chain in amphiphilic copolymers. Furthermore, it is an economical commercial product possessing useful properties such as solubility in aqueous and organic solvents, metal-complexing ability, biological compatibility, nontoxicity, immunity, biodegradability, and ease of chemical modification.[22,23]

Correspondence to: Z. Xu (zushunxu@hubu.edu.cn).
Contract grant sponsor: General Research Funds of the Hong Kong Research Grants Council; contract grant number: CityU 112306.

The synthesis and application of fluorinated polymers have aroused much interest because of their excellent chemical stability, corrosion resistance, anti-oxidation properties, and low surface energy.[24] In fluorinated polymers, most hydrogen atoms at the hydrophobic tail are replaced by fluorine atoms. Although much work has been conducted on the interactions between DNA and amphiphilic copolymers,[25–27] a detailed characterization of the interactions between DNA and fluorinated amphiphilic copolymers is lacking. Coupling amphiphilic copolymers with PEG as the hydrophilic side chain with fluorine-containing hydrophobic backbones is potentially interesting because of the unique properties offered by fluorine-containing materials, such as low surface energy, high contact angles, reduced coefficients of friction, biocompatibility, and hydrophobicity.[28] These desirable properties cannot be easily obtained with nonfluorinated amphiphilic graft copolymers.[29,30] In this work, a novel amphiphilic fluorinated copolymer with hydrophobic poly(hexafluorobutyl methacrylate) backbones and PEG side chains was synthesized, and the relationship between the fluorinated amphiphilic copolymer and DNA were evaluated. The objective was to explore potential applications of fluorinated polymers in biomedical fields.

EXPERIMENTAL

Reagents

2,2,3,4,4,4-Hexafluorobutyl methacrylate (HFMA; Xeogia Fluorine-Silicon Material Co., Harbin, China) was treated by vacuum distillation. Methoxypoly(ethylene glycol)s (MPEGs; Sigma–Aldrich Co., Shanghai, China) with a molecular weight of 2000 were purified via vacuum drying at room temperature for 24 h. Tetrahydrofuran (THF; Shanghai SSS Reagent Co., Shanghai, China) was dehydrated in sodium hydride (Nacalai, Kyoto, Japan) and distilled under reduced pressure. The purity of 4-chloro-α-methylstyrene (Acros Organics Co., Geel, Belgium) reached 95%. 2,2′-Azobis(2-methylpropionitrile) was analytical-grade and was recrystallized in anhydrous ethanol.

A stock solution of calf thymus DNA was prepared by the dissolution of commercially purchased DNA (Sino-American Biotechnology Co., Luoyang, Henan Province, China) in ultrapure water at 0–4°C. The DNA solution concentration was 90 mg/L. Pyrene from Sigma–Aldrich was used to determine the micropolarity of the poly(2,2,3,4,4,4-hexafluorobutyl methacrylate)-*graft*-poly(SPEG) (PHFMA-*g*-PSPEG) solution. All the other reagents were analytical-grade and were made in China. Ultrapure water was used throughout the experimentation.

Apparatus

Fourier transform infrared (FTIR) spectra were obtained from the prepared thin film by means of a KBr pellet on a PerkinElmer (Waltham, MA) Spectrum One instrument. The molecular weight of PHFMA-*g*-PSPEG was determined by gel permeation chromatography (GPC) with a polystyrene standard with a Waters SEC-244 system at 25°C in THF. The ultraviolet–visible (UV–vis) and transmittance spectra were acquired from the PHFMA-*g*-PSPEG solutions on a PerkinElmer Lambda 17 UV–vis spectrophotometer. A high-performance particle sizer (Malvern, MA) was employed to measure the particle size. A WH-2 vortex mixer (Huxi Instrumental Co., Shanghai, China) was used to blend the solution. The resonance light scattering (RLS) spectra and micropolarity measurements were acquired with a Shimadzu (Kyoto, Japan) RF-540 spectrofluorometer. Transmission electron microscopy micrographs were obtained with a JEM-100SX electron microscope (JEOL, Japan).

Methods

Preparation of PHFMA-*g*-PSPEG

MPEG (10.0 g, 2 mmol) was dissolved in dry THF (100 mL), and NaH (0.072 g, 3 mmol) was added by stirring at 45°C for 2 h. Then, 4-chloro-α-methylstyrene (1.22 g, 8 mmol) was added, and the mixture was stirred at 35°C for 24 h. After filtration, 2000 mL of petroleum ether was added to sediment the complex, and a synthesized macromonomer of PEG with double bone in the end was obtained after filtration.

The graft copolymers were synthesized via conventional free-radical polymerization in THF. In a typical reaction, the SPEG macromonomer (0.25 g, 0.0488 mmol), HFMA (0.167 g, 0.6680 mmol), 2,2′-azobis(2-methylpropionitrile) (0.0035 g, 0.0213 mmol), and THF (10 mL) were added to a 50-mL, round-bottom flask equipped with a magnetic mechanical stirrer, well mixed, and polymerized at 75°C for 20 h after vacuum pumping and nitrogen sealing. The product was isolated by evaporation of the solvent in a rotary evaporator, and then the mixture was precipitated in *n*-hexane. After filtration, the precipitate was purified by reprecipitation repeatedly in *n*-hexane. Dried *in vacuo* at 35°C for 72 h, the obtained product was the fluoro-amphiphilic graft copolymer PHFMA-*g*-PSPEG.

Characterization of PHFMA-*g*-PSPEG

The FTIR spectra of SPEG and PHFMA-*g*-PSPEG were obtained with a PerkinElmer Spectrum One instrument after the complex was dried at 25°C *in vacuo*.

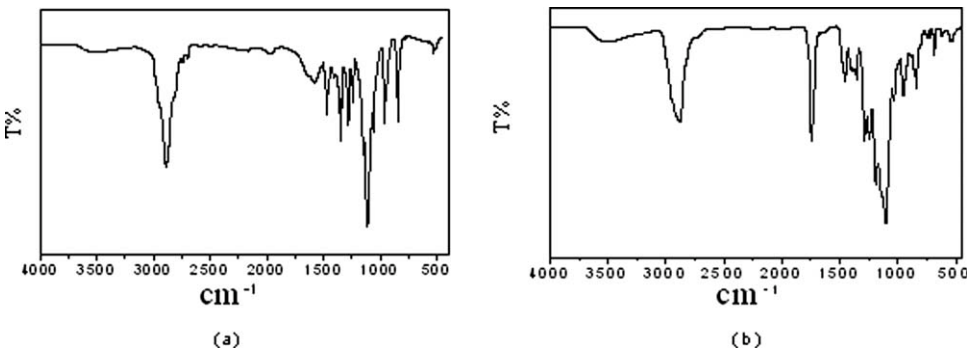

Figure 1 FTIR spectra of (a) the SPEG macromonomer and (b) the PHFMA-*g*-PSPEG copolymer.

^{19}F-NMR spectra were recorded with a Unity Inova 600-MHz spectrometer (Varian, Pala Atto, North Carolina) at 20°C with $CDCl_3$ as the solvent.

The molecular weight of PHFMA-*g*-PSPEG was measured on a Waters 150-C gel permeation chromatograph equipped with polystyrene gel columns (HT2, HT3, and HT4) at 30°C. THF was used as the eluent at a flow rate of 1.0 mL/min, and polystyrene standards were used for calibration.

UV–vis spectroscopy

DNA and PHFMA-*g*-PSPEG were dissolved in ultrapure water and then mixed to obtain various DNA/PHFMA-*g*-PSPEG samples with a constant DNA concentration. The UV–vis spectra were measured with a PerkinElmer Lambda 17 UV–vis spectrophotometer at room temperature. Measurements of absorption were performed in a quartz cuvette (1 cm wide) in the wavelength (λ) range of 200–600 nm, and transmittance measurements were performed in the λ range of 260–700 nm.

Micropolarity

The samples for the fluorescence spectroscopy measurements were prepared in a fashion similar to that for the samples for UV–vis spectroscopy, except that the solvent was a pyrene stock solution obtained by the dissolution of pyrene in pure hot water up to saturation, cooling to room temperature, and finally filtration. The fluorescence spectrum of the mixed solution was recorded on a Shimadzu RF-540 spectrofluorometer at room temperature 1 h after the samples were prepared. A typical emission spectrum (excitation wavelength = 335 nm) of the mixed solution with pyrene as a probe showed five peaks at 374, 378, 384, 394, and 414 nm, and the ratio of the first vibronic peak to the third vibronic peak (I_1/I_3) was sensitive to the local environment (micropolarity) of pyrene.[31,32]

RLS spectroscopy

The DNA and PHFMA-*g*-PSPEG solutions were added to a 25-mL volumetric flask. The mixture was diluted to 10 mL with doubly ultrapure water. After 5 min, the absorption and RLS measurements were taken and referenced to a blank treated in the same way without DNA.

The RLS spectra were obtained by the simultaneous scanning of excitation and emission monochromators on an RF-540 spectrofluorometer in the λ range of 300–600 nm with $\Delta\lambda = 0$ nm. The RLS intensity was measured at the maximum λ value of 422 nm.

RESULTS AND DISCUSSION

FTIR spectroscopy

Figure 1 shows the FTIR spectra of the SPEG macromonomer and PHFMA-*g*-PSPEG. Figure 1(a) shows that the characteristic strong absorption of the hydroxyl group at 3500 cm^{-1} decreased significantly, and the characteristic peak of the double bond at 1640 cm^{-1} could also be observed for the SPEG macromonomer. Those at 3000, 790, and 1800–1400 cm^{-1} for the SPEG macromonomer were the characteristic absorption peaks of the substituent benzene ring. The aforementioned modes confirmed that MPEG was successfully converted into the SPEG macromonomer, which contained the double bond and could act as macromonomer for the synthesis of PHFMA-*g*-PSPEG.

The FTIR spectrum of the PHFMA-*g*-PSPEG copolymer is shown in Figure 1(b). The characteristic absorption of the double bond at 1640 cm^{-1} disappeared, and this indicated that the monomers polymerized. The characteristic stretching peaks of the C=O group strongly appeared at 1700 cm^{-1}, and this resulted from HFMA with C=O groups. In comparison with the FTIR spectra of the SPEG macromonomer, the FTIR absorption peaks at 1000–1260 cm^{-1} were wider and blunter because of the overlap

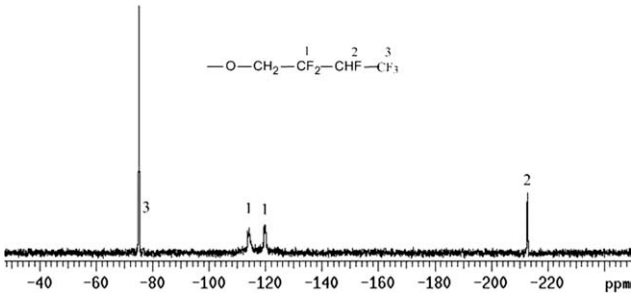

Figure 2 ^{19}F-NMR spectrum of PHFMA-*g*-PSPEG.

of the stretching vibration absorption of the C—F bond at 1100–1260 cm^{-1} with the stretching vibration absorption of the C—O—C bond of the ester groups at 1250 cm^{-1}. This result proved that HFMA and SPEG participated in the polymerization.

To better characterize the structure of the PHFMA-*g*-PSPEG graft copolymer, ^{19}F-NMR was used to determine the fluorocarbon moiety in the copolymer. The ^{19}F-NMR spectrum of the PHFMA-*g*-PSPEG graft copolymer is depicted in Figure 2, and it confirms the presence of three different kinds of fluorine resonances originating from the HFMA side chains. The singlet at −75.2 ppm was assigned to the end —CF_3 group, and that at −212.9 ppm was assigned to the —CHF_2 group. Because of the influence of the —OCH_2— group, the peak of —OCH_2—CF_2— split into two peaks at −114.3 and −119.6 ppm. The ^{19}F-NMR spectrum confirmed that the PHFMA-*g*-PSPEG graft copolymer was successfully prepared.

The molecular weight of the synthesized graft copolymer was measured to be 7131 g/mol by a GPC technique. The GPC results indicated that the reaction of the two monomers occurred, and then the higher molecular weight graft copolymer was obtained.

UV–vis spectroscopy

Figure 3 displays the UV spectra of DNA/PHFMA-*g*-PSPEG. With the addition of the polymer PHFMA-*g*-PSPEG, the absorption of DNA obviously increased, as shown in Figure 3(a). There were three kinds of binding modes between the probe and DNA: electrostatic binding, groove binding, and intercalation binding. The hyperchromic effect resulted from intercalation binding between PHFMA-*g*-PSPEG and DNA base pairs, which changed the conformation of the double-helix structure of DNA.[33] As PHFMA-*g*-PSPEG was a nonionic polymer, there was no electrostatic force between it and DNA. Therefore, the hydrophobic force induced PHFMA-*g*-PSPEG to intercalate to DNA base pairs.

Figure 3(b) shows a weak absorption at 198 nm for PHFMA-*g*-PSPEG, which was assigned to the

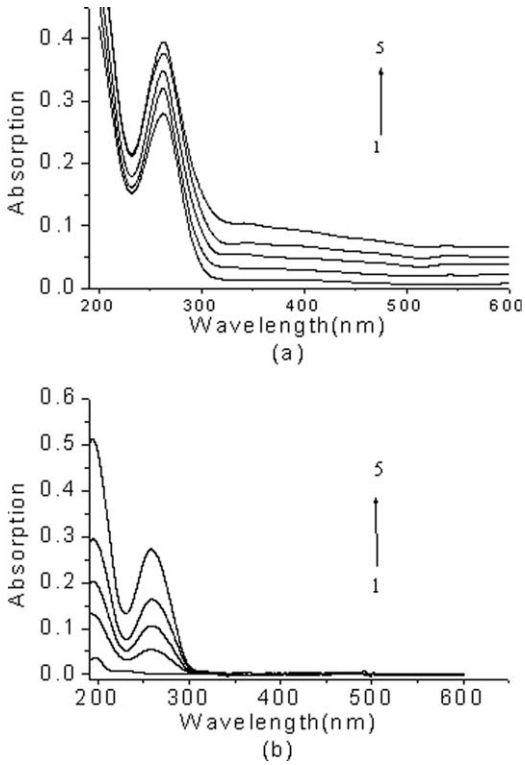

Figure 3 Absorption spectra of (a) DNA [8.0 mg/L DNA and (1) 0, (2) 1.4×10^{-6}, (3) 2.8×10^{-6}, (4) 4.2×10^{-6}, and (5) 5.6×10^{-6} mol/L PHFMA-*g*-PSPEG] and (b) PHFMA-*g*-PSPEG [1.4×10^{-6} mol/L PHFMA-*g*-PSPEG and (1) 0, (2) 2.4, (3) 4.8, (4) 7.2, and (5) 9.6 mg/L DNA].

absorption of a spot of double bonds incompletely synthesized. When DNA was added, there was new absorption at 260 nm, which was the specific absorption of DNA in solution. Besides, the absorption at 198 nm increased, and this indicated that the complex between PHFMA-*g*-PSPEG and DNA had formed.

Figure 4 shows the transmittance as a function of λ measured from DNA/PHFMA-*g*-PSPEG solutions with different PHFMA-*g*-PSPEG concentrations. The

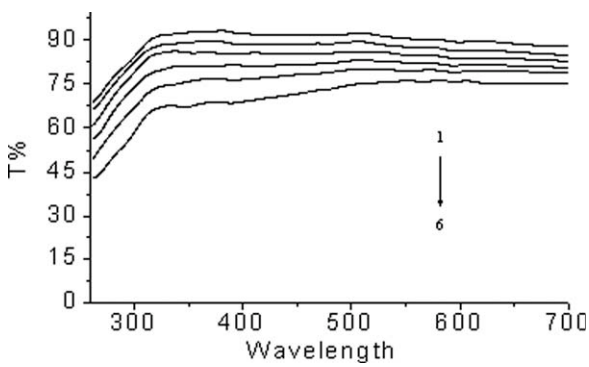

Figure 4 Transmittance (*T*) of the DNA/PHFMA-*g*-PSPEG solutions as a function of λ [17.8 mg/L DNA and (1) 0, (2) 1.4×10^{-6}, (3) 2.8×10^{-6}, (4) 4.2×10^{-6}, (5) 5.6×10^{-6}, and (6) 7.0×10^{-6} mol/L PHFMA-*g*-PSPEG].

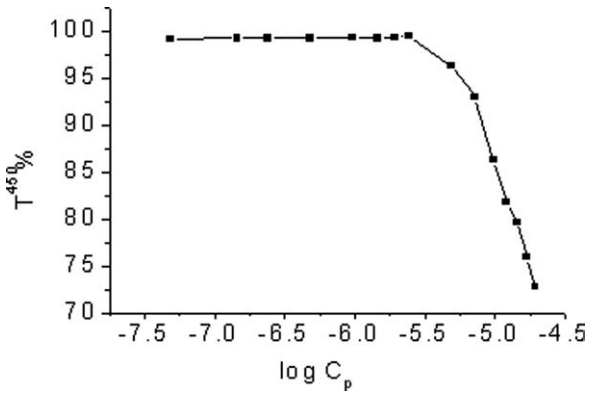

Figure 5 PHFMA-*g*-PSPEG concentration (C_p) dependence of the transmittance at $\lambda = 450$ nm (T^{450}) in the DNA/PHFMA-*g*-PSPEG solutions (17.8 mg/L DNA).

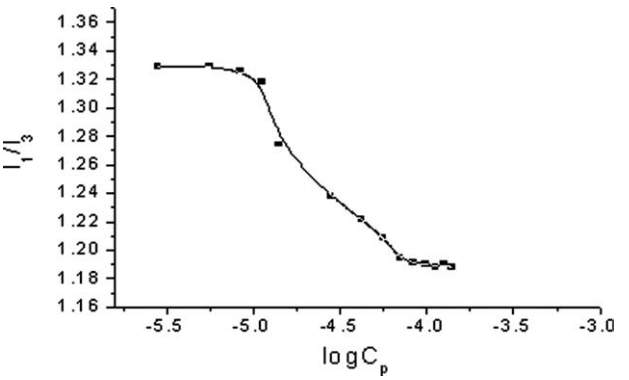

Figure 6 PHFMA-*g*-PSPEG concentration (C_p) dependence of the micropolarity in the PHFMA-*g*-PSPEG solutions.

transmittance had a minimum in the range of 190 nm $< \lambda <$ 300 nm that corresponded to the absorption band of DNA, as shown in Figure 3(a), and it approached approximately 95% of the maximum magnitude when λ was greater than 300 nm. With the addition of PHFMA-*g*-PSPEG, the transmittance decreased. The values of the transmittance at $\lambda = 450$ nm, which were far from the absorption band of DNA, were taken from the measured spectra to examine the PHFMA-*g*-PSPEG effect.[34] Figure 5 shows the polymer PHFMA-*g*-PSPEG concentration dependence of the transmittance at $\lambda = 450$ nm in DNA/PHFMA-*g*-PSPEG. With an increasing concentration of PHFMA-*g*-PSPEG, the transmittance initially was almost constant and then decreased rapidly because of the formation of large DNA/PHFMA-*g*-PSPEG aggregates. The binding of PHFMA-*g*-PSPEG molecules to DNA and the formation of DNA/PHFMA-*g*-PSPEG aggregates arose from the hydrophobic interactions. The amphiphilic copolymer PHFMA-*g*-PSPEG with a fluorine-containing hydrophobic backbone had a strongly hydrophobic nature because substitution of the fluorine atom for hydrogen increased the amphiphilic nature of the polymer and made it more hydrophobic. Therefore, PHFMA-*g*-PSPEG was bound to the base pair of DNA because of the strong hydrophobic interaction of the fluorine-containing hydrophobic chains of PHFMA-*g*-PSPEG. This hydrophobic interaction may have caused more PHFMA-*g*-PSPEG molecules to be cooperatively bound.

Micropolarity

The I_1/I_3 value in a fluorescence spectrum reflects the intensity of the micropolarity around pyrene, and a change in I_1/I_3 can be used to detect the formation of micelles and aggregates in solution. Figures 6 and 7 show the dependence of I_1/I_3 on the PHFMA-*g*-PSPEG concentration in PHFMA-*g*-PSPEG and DNA/PHFMA-*g*-PSPEG solutions, respectively. Figure 6 shows that at a very low PHFMA-*g*-PSPEG concentration, I_1/I_3 was nearly constant, and this implied that no hydrophobic microdomain formed in the solution. As the PHFMA-*g*-PSPEG concentration increased, a sharp decrease in I_1/I_3 reflected the onset of the micelle-like structure, which was defined as the critical micelle concentration. The critical micelle concentration of PHFMA-*g*-PSPEG was 1.12×10^{-5} mol/L. Figure 7 shows a similar phenomenon, but the concentration was lower when I_1/I_3 decreased sharply, and this was defined as the critical aggregation concentration. The critical aggregation concentration of PHFMA-*g*-PSPEG was 7.0×10^{-7} mol/L. Because of the strong hydrophobic interaction between PHFMA-*g*-PSPEG and DNA, the effective concentration of PHFMA-*g*-PSPEG around DNA was lower than that in the bulk, and so the critical aggregation concentration was much lower than the critical micelle concentration in the DNA-free solutions.

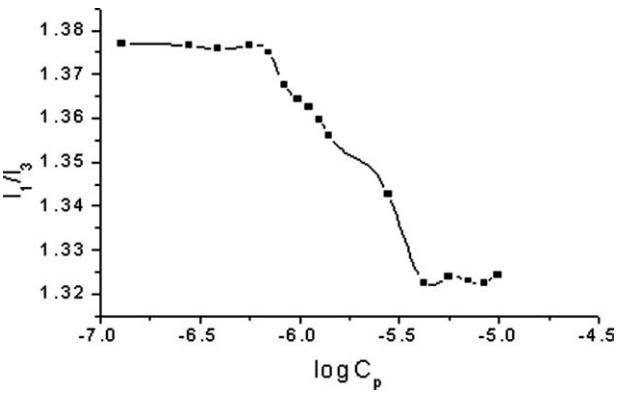

Figure 7 PHFMA-*g*-PSPEG concentration (C_p) dependence of the micropolarity in the DNA/PHFMA-*g*-PSPEG solutions.

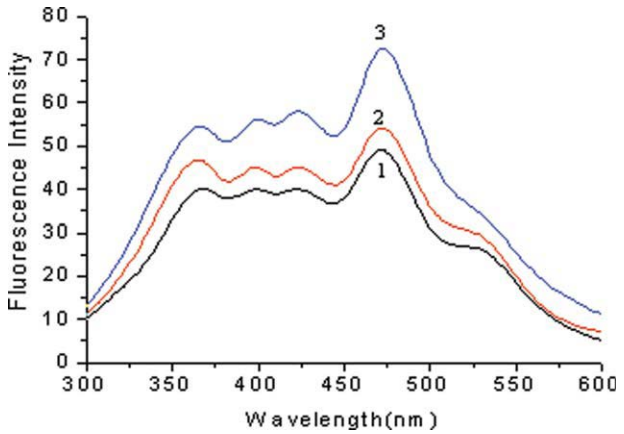

Figure 8 Resonance light scanning of the PHFMA-*g*-PSPEG/DNA solutions [2.8×10^{-6} mol/L PHFMA-*g*-PSPEG and (1) 0, (2) 0.6, and (3) 1.2 mg/L DNA]. [Color figure can be viewed in the online issue, which is available at www.interscience.wiley.com.]

RLS spectroscopy

Figure 8, which was obtained according to the standard procedures, shows that PHFMA-*g*-PSPEG had four weak RLS peaks at 370, 400, 422, and 470 nm. When calf thymus DNA was added, enhanced RLS peaks could be observed at 370, 400, 422, and 470 nm as a result of the long-range assembly of PHFMA-*g*-PSPEG on the molecular surface of nucleic acid.[35] The enhanced RLS peak at 422 nm was the most obvious, and so the RLS intensity was measured at the maximum λ value of 422 nm in our experiments.

The extent to which a particle absorbs and scatters light depends on its size, shape, index of refraction with respect to the surrounding medium, and scattering. Scattering in each sphere is proportional to the square of the volume. The RLS formula is as follows[36,37]:

$$I_{\mathrm{RLS}} = \frac{32\pi^3 V^2 n^2 N}{3\lambda_0^4}[(\delta_n)^2 + (\delta_k)^2],$$

where I_{RLS} is RLS intensity; n is the refractive index of the medium; N is the molarity of the solution; λ_0 is the wavelength of the incident and scattered light; V is the square of the molecular volume; and δ_n and δ_k are the fluctuations in the real and imaginary components of the refractive index of the particle, respectively. When other factors are constant, I_{RLS} is related to the size of the formed particle and is directly proportional to the square of the molecular volume. Therefore, with an increasing molecular volume of the associating complex, intensity (I) is obviously enhanced. Therefore, the amount of scattering is directly proportional to the volume of each sphere: the larger the aggregation is, the greater the scattering is. According to the literature,[35,38,39] when PHFMA-*g*-PSPEG molecules assemble and aggregate on the molecular surface of nucleic acid, long-range assembly results and induces the formation of the superhelical structure of the nucleic acid. When light shines on the superhelical structure of the nucleic acid, resonance occurs. Therefore, because aggregation of PHFMA-*g*-PSPEG on the molecular surface of the nucleic acid produces large particles, strongly enhanced RLS can be observed. This fact is in accordance with the UV–vis spectra. Figure 3(a) shows that with the concentration of PHFMA-*g*-PSPEG increasing, the absorbance of DNA at 260 nm increased. Besides, the absorption also increased when λ was beyond 320 nm. The increase in the absorbance at $\lambda > 320$ nm with the increase in the concentration of FC134 resulted from the formation of compact light scattering particles.[40]

The experiments showed that the enhanced intensity of RLS had a good linear relationship when the concentration of DNA was lower than 1.2 mg/L and the concentration of PHFMA-*g*-PSPEG was in the range of 2.8×10^{-6} to 1.4×10^{-5} mol/L. The effects of different concentrations of PHFMA-*g*-PSPEG on the linear relationship in this range and the related calibration curve are displayed in Table I. When the concentration of PHFMA-*g*-PSPEG was 8.4×10^{-6} mol/L, the linear range and the correlation coefficient of a similar linear regression equation were both best, and the detection limit (3σ) was 4.0 μg/L. Therefore, it could be used to determine DNA with PHFMA-*g*-PSPEG by the RLS technique.

TABLE I
Effects of the Concentration of PHFMA-*g*-PSPEG on the Linear Relationship

Concentration of PHFMA-*g*-PSPEG (mol/L)	Linear range of DNA (mg/L)	Linear regression equation	Correlation coefficient	Detection limit (μg/L)
2.8×10^{-6}	0.45–0.75	$I = 11.27C + 25.85$	0.9957	23.0
5.6×10^{-6}	0.18–0.45	$I = 29.33C + 32.00$	0.9948	9.1
8.4×10^{-6}	0.09–0.90	$I = 67.20C + 35.44$	0.9973	4.0
1.12×10^{-5}	0.18–0.45	$I = 33.33C + 48.50$	0.9635	8.0
1.4×10^{-5}	0.36–1.20	$I = 14.2C + 43.56$	0.9954	18.0

I, RLS intensity; C, concentration of DNA.

Particle size

Figure 9 shows the alteration in the particle size of DNA with different concentrations of PHFMA-*g*-PSPEG. The results revealed that the particle diameter increased when PHFMA-*g*-PSPEG was added. This can be explained by the binding of PHFMA-*g*-PSPEG to DNA, which induced PHFMA-*g*-PSPEG aggregation. Consequently, the DNA changed the conformation, and the particle size became bigger; this was in accordance with the enhanced RLS intensity.

CONCLUSIONS

A novel fluorinated amphiphilic copolymer was synthesized, and a series of experiments were used to investigate and prove the interactions between PHFMA-*g*-PSPEG and DNA. The amphiphilic nonionic polymer was concluded to interact with the base pair of DNA on the basis of the hydrophobic interaction between the fluorine-containing hydrophobic group of the polymer and DNA. Because of the hydrophobic characteristic of the fluorinated segments, PHFMA-*g*-PSPEG easily self-assembles to form a spherical structure. Figure 10 is a schematic representation of the concluded interaction between PHFMA-*g*-PSPEG and DNA. In the hydrophobic core formed by fluorinated segments of the polymer, DNA is embedded on the basis of the hydrophobic interaction, and fluorinated segments in the core interact with the base pair of DNA.

As the rigidity of the C—F bond in PHFMA-*g*-PSPEG causes stiffening of the hydrophobic chain and interactions with other molecules, its interaction with DNA is strong, and it can be used to quantitatively determine the DNA. In comparison with the common fluorometric method using a spectrofluorometer and other substances analyzed with the same RLS technique,[41–45] the limit of detection of 4.0 μg/L with PHFMA-*g*-PSPEG by the RLS technique is very low. It can be concluded that PHFMA-*g*-PSPEG is applicable to the determination of DNA with a high sensitivity. Therefore, the use of PHFMA-*g*-PSPEG with the RLS technique may have widespread applications in the quantification of DNA.

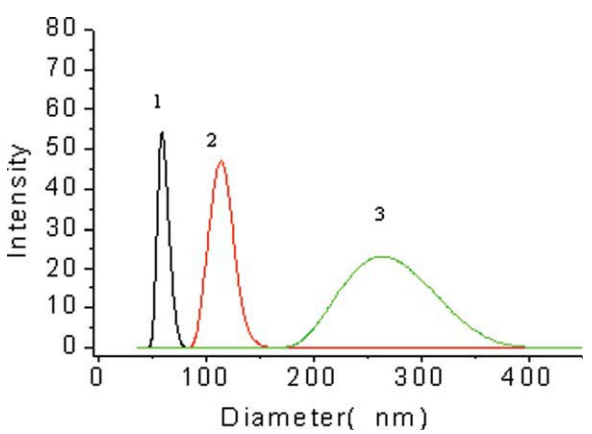

Figure 9 Particle size distribution with a fixed DNA concentration and different concentrations of PHFMA-*g*-PSPEG [2.7 mg/L DNA and (1) 0, (2) 2.0×10^{-6}, and (3) 4.0×10^{-6} mol/L PHFMA-*g*-PSPEG]. [Color figure can be viewed in the online issue, which is available at www.interscience.wiley.com.]

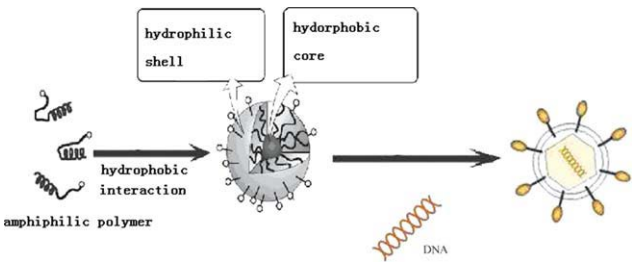

Figure 10 Schematic representation of the PHFMA-*g*-PSPEG and DNA interaction. [Color figure can be viewed in the online issue, which is available at www.interscience.wiley.com.]

References

1. Vincent, K. A.; Shyu, K. G.; Luo, Y.; Magner, M.; Tio, R. A.; Jiang, C.; Goldberg, M. A.; Akita, G. Y.; Gregory, R. J.; Isner, J. M. Circulation 2000, 102, 2255.
2. Williams, J. H.; Sirsi, S. R.; Latta, D. R.; Lutz, G. J. Mol Ther 2006, 14, 88.
3. Lu, Q. L.; Bou-Gharios, G.; Partridge, T. A. Gene Ther 2003, 10, 131.
4. Mahato, R. I.; Smith, L. C.; Rolland, A. Adv Genet 1999, 41, 95.
5. Furgeson, D. Y.; Yockman, J. W.; Janat, M. M.; Kim, S. W. Mol Ther 2004, 9, 837.
6. Lee, M.; Rentz, J.; Bikram, M.; Han, S.; Bull, D. A.; Kim, S. W. Gene Ther 2003, 10, 1535.
7. Huang, S. W.; Wang, J.; Zhang, P. C.; Mao, H. Q.; Zhuo, R. X.; Leong, K. W. Biomacromolecules 2004, 5, 306.
8. Bikram, M.; Ahn, C.; Chae, S.; Lee, M.; Yockman, J.; Kim, S. Macromolecules 2004, 37, 1903.
9. Ahn, C. H.; Chae, S. Y.; Bae, Y. H.; Kim, S. W. J Controlled Release 2002, 80, 273.
10. Lim, Y. B.; Han, S. O.; Kong, H. U.; Lee, Y.; Park, J. S.; Jeong, B.; Kim, S. W. Pharm Res 2000, 17, 811.
11. Zhong, Z.; Song, Y.; Engbersen, J. F.; Lok, M. C.; Hennink, W. E.; Feijen, J. J Controlled Release 2005, 109, 317.
12. Yoo, H. S.; Park, T. G. J Controlled Release 2001, 70, 63.
13. Jeong, B.; Kim, S. W.; Bae, Y. H. Adv Drug Delivery Rev 2002, 54, 37.
14. Bhattacharya, S.; Mandal, S. S. Biochim Biophys Acta 1997, 1323, 29.
15. Wang, Y.; Dubin, P. L.; Zhang, H. Langmuir 2001, 17, 1670.
16. McLoughlin, D.; Langevin, D. Colloids Surf A 2004, 250, 79.
17. Zhao, F. Q.; Huang, L. J.; Zeng, B. Z.; Pang, D. W. Electrochem Commun 2004, 6, 319.
18. Uhríková, D.; Zajac, I.; Dubnicková, M.; Pisárcik, M.; Funari, S. S.; Rapp, G.; Balgavy, P. Colloids Surf B 2005, 42, 59.
19. Lasic, D. D. Liposomes in Gene Delivery; CRC: Boca Raton, FL, 1997.

20. Garnett, M. C. Crit Rev Ther Drug Carrier Syst 1999, 16, 147.
21. Edens, M. W. Nace, V. M., Ed.; Nonionic Surfactant: Polyoxyalkylene Block Copolymers; Marcel Dekker: New York, 1996.
22. Liu, M.; Fu, Z. S.; Wang, Q.; Xu, J. T.; Fan, Z. Q. Eur Polym J 2008, 44, 3239.
23. Li, L.; Zheng, S. X. J Polym Sci Part B: Polym Phys 2008, 46, 2296.
24. Reisinger, J.; Ma, H. Prog Polym Sci 2002, 27, 971.
25. Li, C.; Liu, X.; Meng, L. Z. Polymer 2004, 45, 337.
26. Luu, Y. K.; Kim, K.; Hsiao, B. S.; Chu, B.; Hadjiargyrou, M. J Controlled Release 2003, 89, 341.
27. Dai, F. Y.; Wang, P. F.; Wang, Y.; Tang, L.; Yang, J. H.; Liu, W. G.; Li, H. X.; Wang, G. C. Polymer 2008, 49, 5322.
28. Baradie, B.; Shoichet, M. S. Macromolecules 2005, 38, 5560.
29. Hussain, H.; Budde, H.; Horing, S.; Busse, K.; Kressler, J. Macromol Chem Phys 2002, 203, 2103.
30. Hussain, H.; Busse, K.; Kressler, J. Macromol Chem Phys 2003, 204, 936.
31. Hansson, P. Langmuir 2001, 17, 4161.
32. Hashidzume, A.; Mizusaki, M.; Yoda, K.; Morishima, Y. Langmuir 1999, 15, 4276.
33. Peng, J. F.; Ling, J. Y.; Zhang, H. X.; Zhang, C. K. Spectrosc Spectral Anal 2004, 24, 858.
34. Uhríková, D.; Zajac, I.; Dubničková, M.; Pisárčik, M.; Funari, S. S.; Rapp, G.; Balgavý, P. Colloids Surf B 2005, 42, 59.
35. Huang, C. Z.; Li, Y. F.; Li, N. B.; Luo, H. Q.; Huang, X. H. Chin J Anal Chem 1999, 27, 1241.
36. Anglister, J.; Steinberg, I. Z. J Chem Phys 1983, 75, 443.
37. Anglister, J.; Steinberg, I. Z. Chem Phys Lett 1979, 65, 50.
38. Carvin, M. J.; Fiel, R. J. Nucleic Acids Res 1983, 11, 6121.
39. Huang, C. Z.; Li, K. A.; Tong, S. Y. Anal Chim Acta 1997, 345, 235.
40. Petrov, A. I.; Khalil, D. N.; Kazaryan, R. L.; Savintsev, I. V.; Sukhorukov, B. I. Bioelectrochemistry 2002, 58, 75.
41. Le Pecq, J. B.; Paoletli, C. Anal Biochem 1966, 17, 100.
42. Rye, H. S.; Yue, S.; Wemmer, D. E.; Quesada, M. A.; Haugland, R. P.; Mathies, R. A.; Glazer, A. N. Nucleic Acids Res 1992, 20, 2803.
43. Li, L.; Song, G. W.; Fang, G. R. Am Biotechnol Lab 2007, 25, 34.
44. Jielili, D.; Huang, C. Z. Chin J Anal Chem 1999, 27, 1204.
45. Song, G. W.; Li, L.; Fang, G. R. Can J Anal Sci Spectrosc 2005, 50, 60.